

LITHIUM IN LATE-TYPE GIANTS. I. G AND K GIANTS

DAVID L. LAMBERT AND JAMES F. DOMINY

McDonald Observatory and Department of Astronomy, University of Texas at Austin

AND

SVEIN SIVERTSEN

University of Tromsø, Tromsø

Received 1979 June 18; accepted 1979 July 10

ABSTRACT

Lithium abundances for about 50 G and K giants have been derived from new high-resolution, low-noise spectra by spectrum synthesis. Ca abundances obtained from the 6798 Å Ca I line are well correlated with the [Fe/H] abundance given by published narrow-band photometry. This correlation is strong evidence that the Ca and, therefore, the Li abundances are free from large systematic errors.

The Li abundance and the $^{12}\text{C}/^{13}\text{C}$ ratio are correlated. Red giants with $M \gtrsim 1.3 M_{\odot}$ show the predicted Li abundance and $^{12}\text{C}/^{13}\text{C}$ ratio. Giants with a high ^{13}C abundance ($^{12}\text{C}/^{13}\text{C} \lesssim 15$) show lower Li abundances. It is suggested that Li is a rough measure of a star's mass and that the high ^{13}C stars are low-mass giants $M \lesssim 1.3 M_{\odot}$. The CN cycle is probably the source of the excess ^{13}C . Spallation reactions cannot account for these abundances.

Lithium must be produced by the weak G-band stars. The ^7Be transport mechanism is the probable source of the Li. Meridional mixing in a red giant with a rapidly rotating core occurs too slowly for the ^7Li to be transported to the cool envelope.

Subject headings: nucleosynthesis — stars: abundances — stars: late-type

I. LITHIUM IN STARS

The observed abundance of lithium in stars ranges over more than six orders of magnitude. This fact points to the controlling influence on the Li abundance; i.e., the destruction and production of lithium by nuclear reactions within a stellar interior or on a stellar surface.

Observations of Li in main-sequence stars (Herbig 1965; Zappala 1972) show that Li is depleted relative to the cosmic or interstellar abundance [$\log(\text{Li}) = 3.0$ according to Boesgaard 1976a]. The depletion is most severe in the oldest late-type dwarfs and negligible in the youngest F-type dwarfs. Lithium is destroyed when the convective envelope sweeps material into zones with temperatures $T \gtrsim 10^6$ K. Theoretical calculations of Li depletions are presently unable to account for the observed depletions; the stars are more efficient than their theoretical counterparts in destroying Li (see, however, Schatzman 1977).

Model calculations predict that, at the conclusion of the main-sequence phase, Li is confined to the outermost 1 or 2% (by mass) of the star. When the star evolves up the red-giant branch, the convective envelope grows so that the thin layer containing Li is mixed with a larger mass fraction of Li-free material. Destruction of Li is not predicted in non-rotating stars, but the dilution of the envelope Li cuts the atmospheric abundance by about a factor of 60. In more highly evolved giants, Li may be produced by the sequence $^3\text{He}(\alpha, \gamma)^7\text{Be}(e^-, \nu)^7\text{Li}$. Convection

must remove the ^7Be and ^7Li to cool layers in order to avoid the destruction of the ^7Be and ^7Li by (p, α) reactions; see Cameron (1955) and Cameron and Fowler (1971).

Convective mixing in red giants affects the atmospheric abundances of other light elements and their isotopes. Observations of the $^{12}\text{C}/^{13}\text{C}$ ratio (Lambert 1976; Tomkin, Luck, and Lambert 1976) show that the ^{13}C is enhanced in many G and K giants and supergiants to the predicted level $^{12}\text{C}/^{13}\text{C} \approx 20$ –30. However, other stars show a higher ^{13}C abundance; the ratio $^{12}\text{C}/^{13}\text{C} \sim 4$, which is observed for some stars, is very close to the equilibrium value for the CNO cycle. Theoretical ideas to explain the anomalously low $^{12}\text{C}/^{13}\text{C}$ ratios can be most effectively tested by obtaining accurate abundances for all affected elements and isotopes. In this paper, Li abundances for G and K giants are compared with the $^{12}\text{C}/^{13}\text{C}$ ratios.

The origin of the high ^{13}C abundance is probably the CN cycle. Since exposure of material to the CN cycle also destroys the Li, the simplest schemes for mixing more ^{13}C into an atmosphere produce a simultaneous decrease in the Li abundance. On the other hand, spallation reactions (fast protons or alphas on ^{12}C , ^{14}N , or ^{16}O nuclei) on the stellar surface would increase the Li abundance and the ^{13}C abundance (Audouze 1970; Canal, Isern, and Sanahuja 1978). Wallerstein (1975) noted that the spallation hypothesis could be tested by obtaining Li and ^{13}C abundances for a sample of G and K giants.

Although Li abundances for giants exist in the literature, a new study was begun for three main reasons. First, Li abundances were unavailable for some giants with a high ^{13}C abundance, and the $^{12}\text{C}/^{13}\text{C}$ ratio was unavailable for some giants showing a strong Li resonance line. Second, the Li I resonance doublet at 6707 Å, which is the sole source of a Li abundance in the G and K giants, is generally weak or blended. Therefore, low-noise, high-resolution spectra are an essential prerequisite for an abundance determination. New observations have been obtained for this study. Third, an important goal of this study was to obtain results on Li and the $^{12}\text{C}/^{13}\text{C}$ ratio for a large (~ 50) sample of G and K giants. The Li abundance in an evolved star is controlled by several factors; e.g., stellar mass, main-sequence depletion,

and mass loss. Isolation of the factors is nearly impossible except through careful scrutiny of results for a large sample of giants. Conspicuous exceptions exist, i.e., the Hyades giants for which some information is available on the mass and main-sequence depletion of Li.

II. OBSERVATIONS OF LITHIUM AND CN LINES

High-resolution spectra of G and K giants were obtained with the McDonald Observatory's 2.7 m reflector, the coudé spectrograph, and a Reticon array (Vogt, Tull, and Kelton 1978). One exposure covered about 30 Å at a resolution of about 0.1 Å. Exposures centered near 6707 Å and 6798 Å provided data for the Li I line and a Ca I line, respectively. The

TABLE 1
LITHIUM AND CALCIUM ABUNDANCES

HR	Name	Type	T_{eff}	$\log g$	$^{12}\text{C}/^{13}\text{C}$	$\log \epsilon(\text{Ca})$	$\log \epsilon(\text{Li})$
165.....	δ And	K3 III	4250	2.2	25	6.21	-0.60
168.....	α Cas	K0 II-III	4550	2.1	13	6.04	< -0.6
188.....	β Cet	K1 III	4800	2.9	19	6.60	< -0.3
334.....	η Cet	K3 III	4400	2.7	25	6.22	+0.97
402.....	θ Cet	K0 III	4700	3.0	12	6.08	< -0.4
437.....	η Psc	G8 III	4900	2.7	30	6.21	+1.30
617.....	α Ari	K2 III	4440	2.5	19	6.08	< -0.3
1023.....	...	G0	5000	2.3	2.89
1136.....	δ Eri	K0 IV	4870	3.7	> 50	6.04	+0.75
1346.....	γ Tau	K0 III	4900	2.3	19	6.37	+1.11
1373.....	δ Tau	K0 III	5000	2.8	23	6.48	+0.99
1409.....	ϵ Tau	K0 III	5000	2.8	22	6.48	+0.90
1411.....	θ^1 Tau	K0 III	5000	3.0	20	6.45	+0.86
1457.....	α Tau	K5 III	3790	1.8	12	6.04	< -2.0
1481.....	53 Eri	K2 III	4550	2.9	34	5.90	-0.28
2429.....	ν^2 CMa	K1 IV	4800	3.4	51	6.44	+0.38
2574.....	θ CMa	K4 III	3900	1.9	12	5.84	< -1.0
2985.....	κ Gem	G8 III	4900	3.0	28	6.18	+0.60
2900.....	β Gem	K0 III	4750	2.8	16	6.32	+0.44
3249.....	β Cnc	K4 III	4000	1.9	10	5.94	< -1.5
3748.....	α Hya	K4 III	4100	1.9	18	6.00	-0.33
3905.....	μ Leo	K2 III	4460	2.2	18	6.56	-0.3:
3994.....	λ Hya	K0 III	4900	3.1	17	6.52	+0.78
4094.....	μ Hya	K4 III	3950	1.7	21	6.09	< -1.2
4247.....	46 LMi	K0 III-IV	4700	2.9	22	6.02	+0.09
4301.....	α UMa	K0 II-III	4700	2.5	22	6.51	+1.26
4335.....	4 UMa	K1 III	4500	2.3	32	6.16	+0.95
4377.....	ν UMa	K3 III	4000	1.8	19	5.86	-0.65
4382.....	δ Crt	G8 III-IV	4500	2.6	13	5.80	< -0.55
4608.....	\circ Vir	G8 III	4800	2.8	15	5.83	+0.10
4813.....	χ Vir	K2 III	4350	2.0	28	6.20	-0.20
4924.....	37 Com	G9 II-III	4500	2.25	3.4	6.48	+1.18
4932.....	ϵ Vir	G9 II-III	4950	2.7	20	6.27	+0.09
5068.....	69 Vir	K1 III	4650	2.3	24	6.20	+0.50
5288.....	θ Cen	K0 III-IV	4750	(3.0)	10	6.08	-0.39
5340.....	α Boo	K2 IIIp	4260	1.6	7	5.90	< -1.5
5370.....	20 Boo	K3 III	4400	2.3	23	...	+0.1
5563.....	β UMi	K4 III	4000	2.0	11	5.88	< -1.5
5681.....	δ Boo	G8 III	4990	2.4	15	6.08	+0.90
5854.....	α Ser	K2 III	4470	2.7	14	6.28	-0.28
6705.....	γ Dra	K5 III	3780	1.8	13	5.92	< -1.6
6766.....	...	Gp	4750	2.0	4.1	...	+0.75
6791.....	...	K0 p	5000	2.5	4.5	...	+1.65
7635.....	γ Sge	K5 III	3780	1.4	13	5.88	-1.37
7949.....	ϵ Cyg	K0 III	4750	2.9	11.5	6.02	< -0.1
7957.....	η Cep	K0 IV	4850	3.5	> 30	5.92	+0.35
8694.....	ι Cep	K1 III	4680	2.8	16	6.15	< -0.2
8974.....	γ Cep	K1 IV	4750	3.3	24	6.28	-0.05

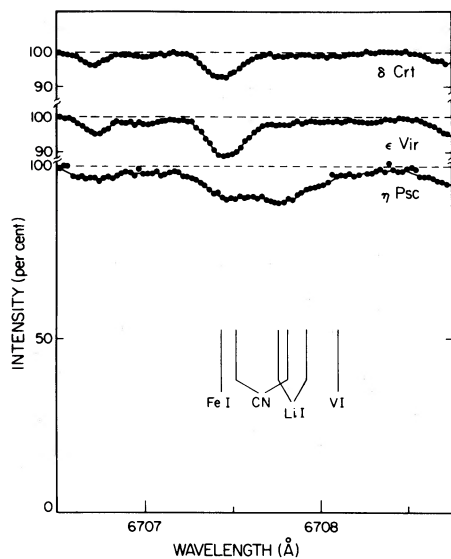


FIG. 1.—The Li I 6707 Å doublet in three G giants. The trio are arranged in order of their $^{12}\text{C}/^{13}\text{C}$ ratio: δ Crt ($^{12}\text{C}/^{13}\text{C} = 13$), ϵ Vir ($^{12}\text{C}/^{13}\text{C} = 20$), and η Psc ($^{12}\text{C}/^{13}\text{C} = 30$). Note the decrease of the Li I intensity with increasing ^{13}C abundance.

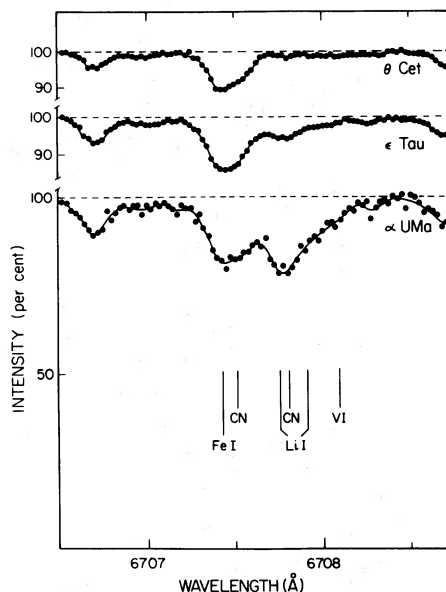


FIG. 2.—The Li I 6707 Å doublet in three K giants. The Li I doublet is strong in α UMa and moderately strong in ϵ Tau. Both stars show the expected ^{13}C and Li abundances (see text). The Li I line is not detectable in θ Cet with a high ^{13}C abundance ($^{12}\text{C}/^{13}\text{C} = 12$). The very weak absorption at the Li I position is provided by CN and other lines.

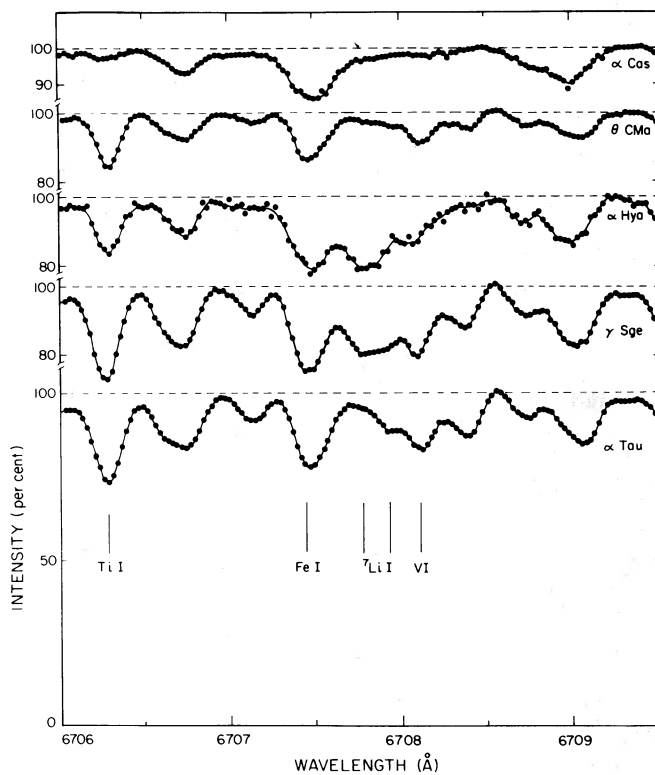


FIG. 3.—The Li I 6707 Å doublet in late-K giants. The spectra of α Cas (K0 II–III), θ CMa (K4 III), and α Tau (K5 III) show how the CN and TiO blends affecting the Li I doublet vary with spectral type; Li I is considered undetectable in all three stars. The comparisons γ Sge/ α Tau and α Hya/ θ Cet show additional absorption contributed by the Li I doublet.

signal-to-noise ratio was typically in excess of 100. Spectra near 8000 Å and 6260 Å which contain CN lines were obtained for a few stars for which the $^{12}\text{C}/^{13}\text{C}$ ratio was not known from earlier work; see Tomkin, Luck, and Lambert (1976) and references therein for details of the $^{12}\text{C}/^{13}\text{C}$ analysis.

The program stars are listed in Table 1. Sample spectra in the Li I region are shown in Figures 1, 2, and 3.

III. THE LITHIUM ABUNDANCE ANALYSIS

A spectrum synthesis-model atmosphere approach to the abundance analysis was adopted. This is a convenient technique because the Li I 6707 Å doublet is often weak and blended. Model atmospheres by Bell *et al.* (1976) were chosen for the spectrum synthesis. Model parameters—the effective temperature and the surface gravity—were generally taken from the published papers which give the $^{12}\text{C}/^{13}\text{C}$ results. In cases where the stellar T_{eff} and $\log g$ did not exactly match those of an available model, the closest model was chosen. The maximum and average differences $|T_{\text{eff}}(\text{model}) - T_{\text{eff}}(\text{star})|$ and $|\log g(\text{model}) - \log g(\text{star})|$ were (120 K, 35 K), and (0.40, 0.20), respectively. The microturbulent velocity was taken from the CN curve-of-growth analyses or set at 2 km s^{-1} . The exact value is not critical because the Li I line is never strongly saturated. The macroturbulent velocity was estimated from line profile fits to one or more of the following lines: Fe I at 6703.57, 6704.48, 6712.47, 6713.75 Å; Ti I at 6716.71 Å. A Gaussian distribution function of macroturbulent velocities was assumed.

The line list for the spectrum synthesis was taken from Luck (1977). The $^{12}\text{CN}(5, 1)R_1(64)$ line is the principal contaminant of the Li I doublet. The intensity of this and other CN lines was set by using unblended CN lines present on the Li I spectrum. TiO contributes several lines to the Li I region in K4 and cooler giants (see Fig. 3). Unblended TiO lines were used to set the TiO lines within the Li I doublet. The Fe I and V I lines to the blue and red, respectively, were set by using the part of their profiles unaffected by the Li I doublet. After the contributions from the various blends had been defined, the Li I lines were added to the line list and a Li abundance was derived. Sample synthetic and observed spectra of ι Cep and β Gem are compared in Figure 4.

The observed spectra of these two stars are identical except for their Li I features. Synthetic spectra for β Gem with $[\log \epsilon(\text{Li}) = 0.44]$ and without Li are shown. Clearly, the Li I doublet is present. On the other hand, the synthetic spectrum without Li fits the ι Cep spectrum quite well so that a Li I doublet is not demanded. Lithium abundances are given in Table 1. When the Li I contribution is less than one-half of the underlying CN and TiO blend, the Li abundance is given as an upper limit.

The possibility of an unidentified blend cannot be dismissed out of hand. There does appear to be a weak unidentified line in the red wing of the Fe I-CN blend at 6707 Å (see Fig. 4). Another very weak line

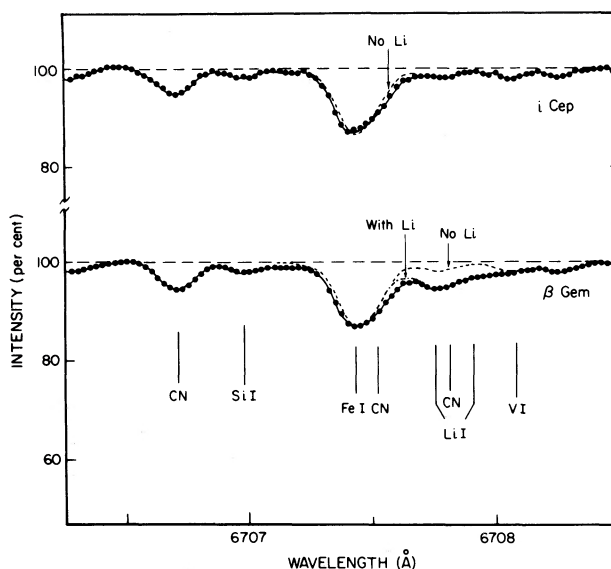


FIG. 4.—Observed and synthetic spectra of ι Cep and β Gem. Li is present in β Gem. Li is absent from the ι Cep spectrum.

appears at 6708.3 Å. Although neither influences the Li I abundance determination, the decision to quote upper limits was based in part upon the possibility of an additional and unidentified blend within the Li I profile.

The lithium is assumed to be ^7Li . Since ^6Li is destroyed more easily than ^7Li , the lithium in a giant is predicted to be ^7Li with only a minor contribution from ^6Li . Unfortunately, the Li I line profile contains little information on the $^7\text{Li}/^6\text{Li}$ ratio. The stronger ^6Li component of the doublet is almost coincident with the weaker ^7Li component. The V I line is superposed on the weaker ^6Li line. For the synthesis of the ψ UMa spectrum where the Li I line is strong, the ^6Li lines were added to the line list. Spectrum synthesis showed no evidence for a ^6Li component. Inspection of spectra of other program stars revealed no cases requiring a ^6Li contribution.

The Ca I line at 6798.5 Å was observed and analyzed in order to provide a check on the Li analysis. The Ca I line follows the Li I quite closely in its predicted dependence on effective temperature and surface gravity (Fig. 5). The predicted equivalent width ratio $R = W_\lambda(\text{Li I})/W_\lambda(\text{Ca I})$ is insensitive to $\log g$ but displays a modest sensitivity to T_{eff} ($\Delta \log R \approx 0.06$ for $\Delta T_{\text{eff}} = 100 \text{ K}$). The ratio $S = W_\lambda(\text{Li I})/W_\lambda(\text{Fe I})$ for one of the Fe I lines, which are observed in the Li I and Ca I echelle spectra, shows a greater dependence on both $\log g$ and T_{eff} . Clearly the Ca I line is the better comparison for Li I.

The Ca I line is affected by two weak blends. A CN line—(7, 3) $P_1(30)$ at 6798.364 Å—is in the blue wing of the 6798.479 Å Ca I line profile. A Cr I line at 6798.439 Å (Kurucz and Peytreemann 1975) is not a significant contributor; a stronger line of the same multiplet is very weak. In the cooler stars, TiO

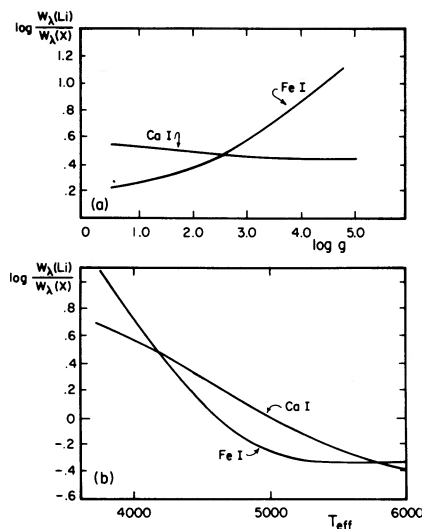


FIG. 5.—Variation of the equivalent width of the Li I doublet relative to the Ca I 6798 Å and a representative Fe I line. Panel (a) shows the variation with $\log g$ for $T_{\text{eff}} = 4250$ K. Panel (b) shows the variation with T_{eff} for $\log g = 2.25$.

provides blending lines. The CN and TiO contributions were assessed by using neighboring lines of these molecules. The Ca I line is weak to moderately strong in the program stars: $20 < W_\lambda < 40$ mÅ. The corrected equivalent width was used for the Ca abundance analysis.

The gf -value of $\log gf = -2.44 \pm 0.05$ (Smith 1978) for the 6798 Å Ca I line is based on solar relative gf -values as well as accurate relative gf -values obtained with the Oxford furnace [the new measurements are an extension of work reported by Smith and O'Neill (1975)]. The absolute scale of the relative gf -values is set by the radiative lifetime measurement (Gornik *et al.* 1973) of the $3d4p\ ^1F$ level. The new gf -values provide a solar Ca abundance which is in excellent agreement (Smith 1978) with the abundance recommended by Lambert and Luck (1978) on the basis of the Ca I 6572 Å intercombination resonance line and the Ca II permitted and forbidden lines. Lambert and Luck noted that the Ca I gf -value available to them led to an apparently discrepant Ca abundance. This discrepancy has vanished.

The current stellar sample covers a modest range in metallicity. In Figure 6, the Ca abundance from the 6798 Å line is plotted against the iron abundance [Fe/H] obtained from narrow-band photometry of Williams (1971, 1972*a, b*), Hansen and Kjaergaard (1971), and Gustafsson, Kjaergaard, and Andersen (1974). The recipe provided by Branch (1979) was used to construct mean [Fe/H] values on the Hansen and Kjaergaard scale. There is a good correlation between the independent Ca and Fe abundance estimates. The [Ca/Fe] index constructed from Figure 6 is shown in Figure 7 as a function of effective temperature. The raw abundance $\log \epsilon(\text{Ca})$, which is also plotted, shows an increased scatter at a fixed T_{eff} . This scatter is

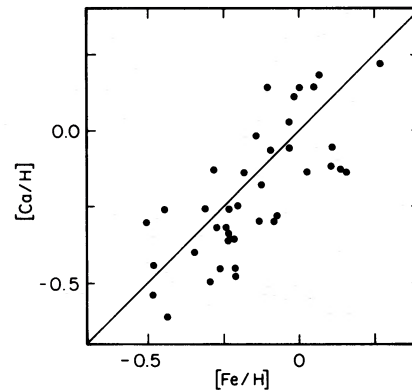


FIG. 6.—[Ca/H] and [Fe/H] for the present sample. [Ca/H] is obtained from Table 1 using $\log \epsilon(\text{Ca})_\odot = 6.34$. [Fe/H] is obtained from narrow-band photometry—see text. Note $[X] = \log X_{\text{star}} - \log X_\odot$.

attributable to the spread in the metallicities. The absolute Ca abundance appears to be normal (i.e., $[\text{Ca}/\text{Fe}] \approx 0$) across the range of T_{eff} . There is a hint that [Ca/Fe] decreases at the lower end of the T_{eff} range; say $[\text{Ca}/\text{Fe}] \sim -0.15$ at $T_{\text{eff}} \sim 4000$ K. Note that a ± 250 K error in T_{eff} produces a ∓ 0.20 dex error in the Ca abundance at $T_{\text{eff}} \sim 4500$ K. The Ca abundance is quite insensitive to the adopted $\log g$: ± 1.5 dex in $\log g$ at $\log g = 2.25$ produces an error of less than ∓ 0.02 dex in the abundance.

Since Ca and Li are similar atoms, the Ca abundances indicate that the Li abundances are not seriously affected by systematic errors. The Li abundance is more temperature sensitive than the Ca abundance (see Fig. 5): a ± 250 K error at $T_{\text{eff}} = 4500$ K produces a ∓ 0.35 dex error in the Li abundance. The Ca abundances indicate that a T_{eff} related error in the Li abundance cannot be larger than ± 0.25 dex. If the T_{eff} errors are random, the mean Li abundance will be reduced for the sample and subsets of the sample. The T_{eff} error is the major uncertainty for some stars. When the Li I doublet is weak, the largest error arises in the correction for the CN/TiO blends. Fortunately, the Li abundance ranges over four orders of magnitude so that interesting

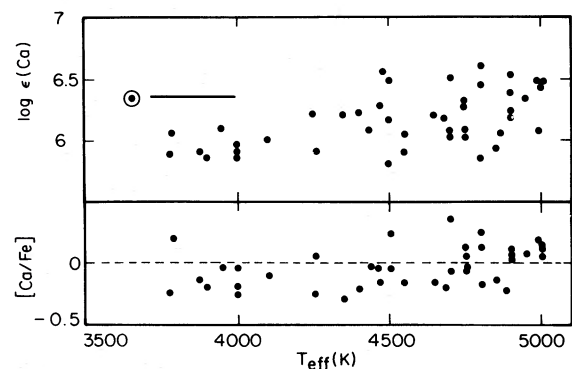


FIG. 7.—Calcium abundances as a function of effective temperature: $\log \epsilon(\text{Ca})$: top panel; [Ca/Fe]: bottom panel.

conclusions may be drawn in spite of an error of about ± 0.3 dex.

The T_{eff} related error would be reduced by about one-half by quoting the results as a Li/Ca abundance ratio. However, the initial Li/Ca ratio of a star is likely to change with the Ca abundance. This is certainly true if the ${}^7\text{Li}$ has a cosmological origin because the initial Li abundance would have been the same for all stars, but the Ca abundance spans about 0.6 dex. On the other hand, if the ${}^7\text{Li}$ is created by galactic cosmic rays or red giants (Reeves 1974), ${}^7\text{Li}$ increases as Ca increases through the Galaxy; the precise form of the Li/Ca ratio with Ca abundance is uncertain. Clearly then, the use of the Li/Ca ratio may introduce an additional uncertainty.

The Li abundances are plotted against T_{eff} in Figure 8. A trend to lower abundances at lower T_{eff} is apparent. There is also a very large range in the abundance for a fixed T_{eff} . The trend and the range cannot be attributed to simple errors in the analysis such as incorrect assignment of T_{eff} . All such errors would affect the Ca abundances; Figure 7 shows no evidence for systematic errors. The form of the Li abundance distribution in Figure 8 is not a new result; Bonsack's (1959) initial survey led to the same result. They must be attributed to a real variation in the Li abundance. Possible origins of the variation are discussed in § IV.

Perhaps the leading potential source of a systematic error in the Ca or Li abundances is the assumption of LTE for the ionization equilibrium. Auman and Woodrow (1975) predict a substantial overionization of the easily ionized metals in cool stellar atmospheres. Ramsey (1977) obtains observational confirmation of their predictions for Ca in cool giants. The warmest star in his small sample was α Tau. The degree of

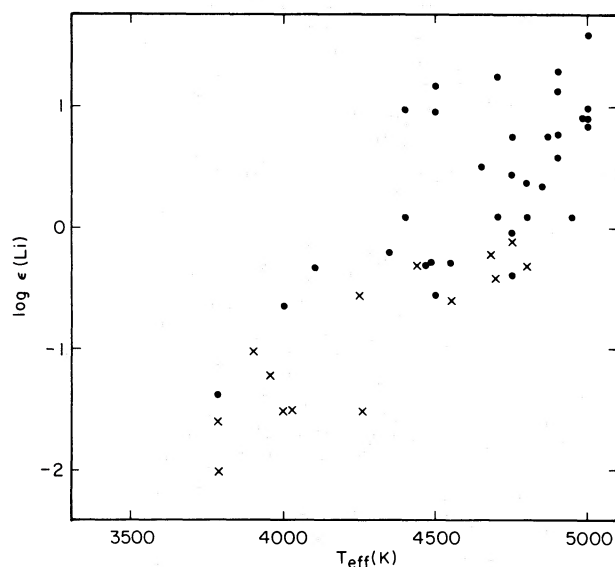


FIG. 8.—Lithium abundances as a function of effective temperature. *Filled circles:* abundance determinations; *crosses:* upper limits.

overionization is predicted to decrease in the hotter G and K stars comprising the present sample. Inspection of Figure 7 shows that the Ca abundance may show a slight decrease with decreasing T_{eff} . (It should be noted that departures from LTE in the Ca I excitation can affect the present abundances but are likely to have only a minor influence on Ramsey's analysis.) Of course, the possible trend in the Ca abundance may be due to effects other than departures from LTE; for example, deficiencies in the model atmospheres related to T_{eff} or a systematic error affecting the T_{eff} values.

Statistical equilibrium calculations for the ionization of Li were reported by Luck (1977); for example, he finds that the overionization in a $T_{\text{eff}} = 4000$ K and $\log g = 1.5$ supergiant model atmosphere corresponds to a $+0.6$ dex correction to an LTE abundance analysis. The coolest stars in the present sample have a surface gravity $\log g \sim 1.9$ for which the correction is perhaps $+0.5$ dex. This is probably an upper limit to a correction because Luck did not allow for line blanketing which decreases the intensity of the ionizing radiation and reduces the departures from LTE. The Li calculations should give an approximate idea of the effect on Ca. Luck's predictions would overcorrect the Ca abundances for the possible trend with T_{eff} .

IV. LITHIUM AND CONVECTIVE MIXING

a) Li and the ${}^{12}\text{C}/{}^{13}\text{C}$ Ratio—Predictions

Surface abundances of the light elements in a red-giant atmosphere are predicted to change as the convective envelope dilutes the pristine material in the outer envelope with material which was partially processed through the CNO-cycle during the main-sequence phase. This mixing is complete before the red-giant tip is reached on the first ascent of the giant branch. A second mixing can occur on the second ascent—the asymptotic giant branch. Observational evidence for the mixing is contained in the abundances of Be (Boesgaard and Chesley 1976; Boesgaard, Heacox, and Conti 1977), Li (Wallerstein 1966; Herbig and Wolff 1966; Wallerstein and Conti 1969; Boesgaard 1971; Alschuler 1975; Luck 1977), the ${}^{12}\text{C}/{}^{13}\text{C}$ ratio (Lambert 1976; Tomkin, Luck, and Lambert 1976), and the C, N, and O abundances (Lambert and Ries 1977; Luck 1978). The observations are not yet fully explained by the stellar evolution calculations.

Different elements and isotopes display differing sensitivities to the several factors controlling nucleosynthesis in the stellar interior and its effect on surface abundances. Hence, observations yield maximum information when several abundances are compared for a sample of giant stars. Here, discussion is centered on the Li abundance and the ${}^{12}\text{C}/{}^{13}\text{C}$ ratio.

Li abundances and measurements of the ${}^{12}\text{C}/{}^{13}\text{C}$ ratio are plotted in Figure 9. Supergiant observations (Luck 1977) are included; note that the Li abundances for the supergiants include the correction for departures from LTE. Figure 9 does not include stars for which Luck provided upper limits to the Li abundance.

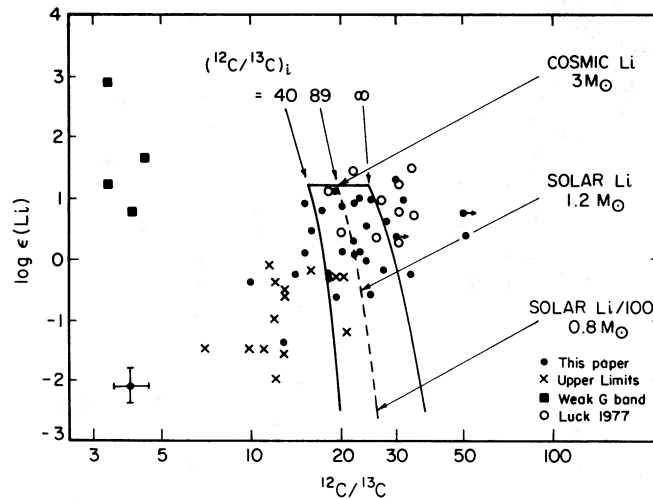


FIG. 9.—The lithium abundance and the $^{12}\text{C}/^{13}\text{C}$ ratio for G and K giants and supergiants. Li abundance determinations are plotted for G and K giants (this paper: *filled circles*), weak G-band giants (this paper: *filled squares*), and G and K supergiants (Luck 1977: *open circles*). Upper limits to the Li abundance for stars in the present sample are given by crosses. Error bars corresponding to ± 0.30 dex in $\log \epsilon(\text{Li})$ and ± 0.06 dex in the $^{12}\text{C}/^{13}\text{C}$ ratio. Theoretical predictions (see text) for standard red-giant models are given for 3, 1.2, and $0.8 M_{\odot}$ stars. The base of each arrow denotes the Li abundance and the $^{12}\text{C}/^{13}\text{C}$ ($= 89$) ratio at the end of the main-sequence phase. The head of the arrow denotes the composition at the top of the red-giant branch. The displacement of the arrowhead for a change of initial $^{12}\text{C}/^{13}\text{C}$ ratio is indicated.

Discussion of Figure 9 should commence with a comparison of the observations and predictions for the nonrotating red giant modeled by standard computer codes. The assumption is made that the initial Li abundance is approximately the same for all stars in the sample; however, the gross conclusions are not dependent on this assumption. The Li abundance in the giant is reduced through dilution. Iben (1965) predicts for a $3 M_{\odot}$ star a reduction by a factor of 60. At $1 M_{\odot}$, the reduction factor is 28 (Iben 1967*a, b*; see also Iben 1966). These dilution factors refer to a star at the tip of the red-giant branch. As noted in § I, Li depletion during the main-sequence phase is not understood in a quantitative sense. However, observations and/or theory show that Li is not depleted in the atmospheres of the more massive stars (say $m \gtrsim 2 M_{\odot}$). If the predicted profile of the Li abundance with depth into the star is correct, these stars as red giants are predicted to have a Li abundance which is a factor of 60 below the initial abundance taken here to be $\log \epsilon(\text{Li})_i = 3.0$ (Boesgaard 1976*a*); i.e., $\log \epsilon(\text{Li}) = 1.2$ for the red giant. This is the predicted upper limit for Li in normal red giants.

Li depletion on the main sequence is observed to increase with decreasing mass. The observations are consistent with the relation

$$\epsilon(\text{Li})_{\text{PMS}} = \epsilon(\text{Li})_i f(m), \quad (1)$$

where $\epsilon(\text{Li})_{\text{PMS}}$ is the post-main-sequence Li abundance prior to dilution as a red giant, and the function $f(m)$ decreases monotonically with decreasing mass. If the Li abundance is assumed to decline exponentially with time for a given star, the time scale is $\tau_{\text{Li}} \sim 1-2 \times 10^9$ years from (i) comparisons of the Li

abundance in galactic clusters of different ages and (ii) a comparison of the meteoritic and solar photospheric Li abundance (Herbig 1965; Zappala 1972). The reasonable agreement between methods (i) and (ii) suggests that τ_{Li} may be nearly mass independent for $m \gtrsim 1 M_{\odot}$. Zappala suggests that τ_{Li} is smaller for stars less massive than the Sun. On the assumption that the Li depletion is exponential over the entire main-sequence lifetime, equation (1) may be written

$$\epsilon(\text{Li})_{\text{PMS}} = \epsilon(\text{Li})_i \exp(-\tau_{\text{MS}}(m)/\tau_{\text{Li}}). \quad (2)$$

The implications of equations (1) and (2) are clear: the Li abundance of a red giant is a measure of the mass of the star. The general result represented by equation (1) is more secure than the specific calibration given in equation (2). Of course, certain key assumptions have to be made. These include the assumption that the models predict correctly the mass of the Li-rich skin in the main-sequence star. The mass-loss rate is assumed to be negligible. It may be noted that there is little direct observational evidence on the severity of the Li depletion process in the latter part of the main-sequence phase. The reasons for the lack of evidence are simple. The Li abundance is reduced to such an extent that the resonance line is not detectable. Modest Li depletions occur in the warmer stars in which Li is largely ionized. Severe Li depletions occur in the cooler stars.

An interesting prediction is obtained by combining equation (2) with the mean red-giant mass, $0.8 M_{\odot} < \langle M_{\text{RG}} \rangle < 1.2 M_{\odot}$, obtained by Scalo, Dominy, and Pumphrey (1978). If $\langle M_{\text{RG}} \rangle = 1.2 M_{\odot}$, the main-sequence lifetime $\tau_{\text{MS}}(1.2 M_{\odot}) \approx 4 \times 10^9$ yr (see, for

example, Miller and Scalo 1979, Table 1). This is close to the present age of the Sun so that

$$\frac{\epsilon(\text{Li})_{\text{PMS}}}{\epsilon(\text{Li})_{0.1.2M_{\odot}}} \approx \frac{\epsilon(\text{Li})_{\text{NOW}}}{\epsilon(\text{Li})_{\text{O}_{\odot}}} = \frac{1}{100},$$

where the depletion of the Li in the Sun is taken to be 10^{-2} (Boesgaard 1976a). The Li in the $1.2 M_{\odot}$ red giant is further diluted below the solar value by a factor of 43 (Iben 1967a, b) at the red-giant tip, i.e., $\log \epsilon(\text{Li}) \approx -0.6$ is predicted. If the lower value for $\langle M_{\text{RG}} \rangle = 0.8 M_{\odot}$ is taken, the main-sequence depletion is increased [$\tau_{\text{MS}}(0.8 M_{\odot}) \approx 17 \times 10^9$ yr] by a factor of nearly 50 over the current solar value to $\log \epsilon(\text{Li})_{\text{PMS}} \approx -0.7$ and dilution in the red giant decreases this to $\log \epsilon(\text{Li})_{\text{RG}} \approx -2.2$. Then, the mean Li abundance in red giants should lie between $\log \epsilon(\text{Li}) \approx -0.6$ and -2.2 .

The ^{13}C enhancement in normal red giants was predicted first by Iben (1964). Predictions have been taken from Dearborn, Tinsley, and Schramm (1978). The red giant $^{12}\text{C}/^{13}\text{C}$ ratio depends on the mass and the initial ($^{12}\text{C}/^{13}\text{C}$)_i ratio; e.g., $^{12}\text{C}/^{13}\text{C} = 18$ ($10 M_{\odot}$) to 25 ($1 M_{\odot}$) for ($^{12}\text{C}/^{13}\text{C}$)_i = 89 and $^{12}\text{C}/^{13}\text{C} = 14$ to 19 for ($^{12}\text{C}/^{13}\text{C}$)_i = 40.

b) Li and the $^{12}\text{C}/^{13}\text{C}$ Ratio in Giants

The predictions for Li and the $^{12}\text{C}/^{13}\text{C}$ ratio are compared with the observations in Figure 9. As discussed, the more massive giants and the young supergiants are expected to lie along a line $\log \epsilon(\text{Li}) \approx 1.2$ and $^{12}\text{C}/^{13}\text{C} \approx 15$ –20. Inspection of Figure 9 shows that indeed this line defines the upper boundary of the sample. The stars with the predicted $^{12}\text{C}/^{13}\text{C}$ ratio extend in Figure 9 down to about $\log \epsilon(\text{Li}) \sim -0.8$; one star (μ Hya) falls below this limit. According to the discussion of equations (1) and (2), this limit corresponds to a mass $m \sim 1.2 M_{\odot}$.

Perhaps the most interesting new result from Figure 9 is the location of the low $^{12}\text{C}/^{13}\text{C}$ stars (the exceptional weak G-band stars are discussed later). The straightforward application of (1) and (2) provides a mass estimate for the low $^{12}\text{C}/^{13}\text{C}$ (<15, say) stars. These stars have Li abundance $\log \epsilon(\text{Li}) \lesssim 0.0$, which translates to $m < 1.3 M_{\odot}$. This limit is consistent with Scalo and Miller's (1978) estimate that $m \lesssim 1.5 M_{\odot}$ for the low average $^{12}\text{C}/^{13}\text{C}$ star. Their argument, which was based on the frequency distribution of the $^{12}\text{C}/^{13}\text{C}$ ratio, sets a crucial constraint on theories to explain the origin of the high ^{13}C abundance.

Spallation reactions on the stellar surface could produce excess ^{13}C , but a high Li would also result. Therefore, spallation must be rejected as the origin of the low $^{12}\text{C}/^{13}\text{C}$ stars.

The excess ^{13}C is almost certainly the product of the CN cycle. The ^{13}C could be added after the Li dilution in a low-mass red giant has gone to completion. If weakly exposed CN-cycled material is then added with $^{12}\text{C}/^{13}\text{C} \sim 4$, no significant ^{12}C depletion, and a negligible Li abundance, the star moves to a

lower Li abundance and a lower $^{12}\text{C}/^{13}\text{C}$ ratio in Figure 9. These assumptions provide a decrease $\Delta \log \epsilon(\text{Li}) \sim 0.6$ as $^{12}\text{C}/^{13}\text{C}$ is reduced from 25 to 5. In this simple model, the modest Li decrease relative to the total spread in Figure 9 requires that the progenitors of the low $^{12}\text{C}/^{13}\text{C}$ stars are normal red giants with $m \sim 1.2$ – $0.8 M_{\odot}$. Sweigart and Mengel (1979) propose that meridional circulation in the interior of a red giant with rapid internal rotation can result in substantial CN processing. Inspection of their paper suggests that Li will be destroyed by such meridional circulation. Hence, their scheme appears to explain the decrease of Li with increasing ^{13}C abundance. However, their models do not appear to be capable of explaining Li in the weak G-band stars (see below).

The Li abundance in giants is moderately well correlated with effective temperature (Fig. 8). This appears to reflect two facts: (i) the Li abundance is correlated with stellar mass [eqs. (1) and (2)]. Since T_{eff} is lower for the lower mass stars, which destroy more Li on the main sequence, low T_{eff} implies a lower Li abundance; (ii) examination of the absolute luminosities shows that the low Li and high ^{13}C stars are predominantly the higher luminosity members of the sample. Since the red-giant branches of a stellar evolution track show T_{eff} to decrease as luminosity increases, a concentration of low Li and high ^{13}C stars toward high luminosity provides a correlation of the Li and the $^{12}\text{C}/^{13}\text{C}$ ratio with T_{eff} . Along the first ascent of the red-giant branch, Li steadily decreases as dilution occurs. However, this is probably not a major contributor to the correlation. The initial decrease near the base of the red-giant branch brings the Li dilution close to the final value. Furthermore, a star spends more time on the second ascent so that the great majority of stars in the sample should have experienced the maximum dilution of Li.

Identification of an approximately unique relation between Li abundance and stellar mass may help to explain the $^{12}\text{C}/^{13}\text{C}$ –metal abundance correlation (Branch 1979). The average age of giants must increase with decreasing mass. The average metal abundance is also expected to decrease with decreasing mass. Therefore, the correlation of low $^{12}\text{C}/^{13}\text{C}$ ratio with low metal abundance probably reflects the appearance of low $^{12}\text{C}/^{13}\text{C}$ ratio in the lower mass stars.

A more demanding test of the Li and $^{12}\text{C}/^{13}\text{C}$ predictions is possible when the mass of the red giant is known. The Hyades giants offer this possibility: $m = 2.0 \pm 0.3 M_{\odot}$ according to van den Heuvel's (1975) estimate of the mass at the main-sequence turnoff. The Li abundance at the turnoff is $\log \epsilon(\text{Li}) = 2.9$ according to Zappala (1972). The mean abundance for the four giants is $\log \epsilon(\text{Li}) = 1.0$ or a dilution factor of $10^{1.9} = 79$. The predicted dilution factor for a giant after reaching the tip of the first red-giant branch is 60. The agreement is satisfactory in view of the abundance uncertainties for both the giants and the main-sequence stars.

Li abundances were determined earlier by Boesgaard

(1970). Her results are about a factor of 2 smaller than present values. In part, this difference reflects differences in the assigned effective temperatures. With the lower Li abundances, Boesgaard, Heacox, and Conti (1977) noted a factor of 2 discrepancy between the observed and predicted red-giant Li abundance which they attributed to mass loss: $0.02 M_{\odot}$ prior to the red-giant phase. The new Li abundances require less mass loss. Both mass-loss estimates are subject, of course, to the qualification that the theoretical prediction for the depth of the Li-containing zone be correct.

Another measure of mass loss is provided by the sample of Ib stars analyzed by Luck (1977). These stars have masses in the range $5\text{--}12 M_{\odot}$ and main-sequence progenitors of spectral type B0–B5. Lithium is not observable in these hot main-sequence stars. Li abundances have been derived for main-sequence stars (Herbig 1965; Zappala 1972) up to F0 where a negligible depletion is found. Extrapolation to B0 by using the theoretical models of Bodenheimer (1965) suggests that Li is not depleted in the atmospheres of these stars. Hence, the Li in the Ib stars should be decreased by a factor of 60 below the initial or cosmic abundance. Three of the Ib stars with a normal $^{12}\text{C}/^{13}\text{C}$ ratio have a Li abundance nearly a factor of 10 below the predicted abundance. A modest amount of mass loss (roughly 2% of the stellar mass in the main-sequence lifetime or $10^{-8} M_{\odot} \text{yr}^{-1}$ for a $9 M_{\odot}$ star) could account for this reduced Li abundance. Unless the mass loss is extremely severe, the Li abundance is cut without a significant change of the $^{12}\text{C}/^{13}\text{C}$ ratio.

c) Main-Sequence Problems

Predictions for Li and the $^{12}\text{C}/^{13}\text{C}$ ratio in giants are dependent on assumptions about the structure of the main-sequence stars. The Li predictions are sensitive to the adopted mass for the Li-rich outer skin. Since theoretical calculations do not achieve the correct Li depletion on the main sequence, there is a concern that the predicted mass of the Li-rich skin may also be in error. Calculations by Weymann and Sears (1965) done for a variety of solar models show only modest changes in the mass of the skin. This is some evidence that variations in the mass of the skin have a minor effect in Figure 9.

Observations of beryllium in main-sequence stars shed additional light on main-sequence depletion of light elements. Be is not normally depleted on the main sequence. In some of the hotter ($T_{\text{eff}} > 6600$ K) stars, Boesgaard (1976b) has discovered remarkable Be deficiencies. Li also appears to be overdeficient in these stars; it would be surprising if Li deficiencies did not accompany the Be deficiencies which amount to a factor of 10 or more. In her sample, about one in three of the main-sequence stars with $T_{\text{eff}} > 6600$ K showed the Be deficiency. If the abundance profile of Li within these stars is similar to that in the normal stars of the same T_{eff} which do not deplete Li on the main sequence, the Be-deficient stars will

evolve into Li-poor red giants with an abundance $\log \epsilon(\text{Li}) \lesssim 0.2$; i.e., a factor of 10 (or more) below the upper limit for red giants.

The present sample may contain a few such stars. Since the Li and Be overdepletion could be produced without additional CN processing, the Be-deficient stars probably have a normal $^{12}\text{C}/^{13}\text{C}$ ratio as a giant. Mu Hya with $\log \epsilon(\text{Li}) < -1.2$ and $^{12}\text{C}/^{13}\text{C} = 21$ is a possible example. This discussion has assumed that the Be and Li deficiencies result from a destruction of these elements. If the lower atmospheric abundance results from diffusion (Vauclair *et al.* 1978), the abundances in the red giant are likely to be normal. It may be possible by examining Li and Be abundances in a large sample of giants to distinguish between the destruction and diffusion assumptions.

d) Subgiants

The present sample must contain a few stars which have not evolved to the tip of the red-giant branch. In these cases, the Li and the $^{12}\text{C}/^{13}\text{C}$ ratios will be changed by smaller amounts from the initial values. Stars falling to the right of the $(^{12}\text{C}/^{13}\text{C})_i = \infty$ locus in Figure 9 are in this category. Two subgiants— δ Eri and ν^2 CMa—are obvious examples. Their high $^{12}\text{C}/^{13}\text{C}$ ratio and position in the H-R diagram suggest that convective mixing has not ceased. Depletion of Li and Be in subgiants has been discussed by Herbig and Wolff (1966) and Boesgaard and Chesley (1976).

The observed Li abundance for δ Eri is consistent with the Li abundance of the F7 dwarf which was the main-sequence progenitor according to the stellar evolutionary tracks. Boesgaard and Chesley note that Li is predicted to be depleted by a factor of 7 in δ Eri. With this factor, the predicted main-sequence abundance is $\log \epsilon(\text{Li}) = 1.6$ which is close to the lower end of the observed distribution (Herbig 1965) for F7 dwarfs. The dwarfs contributing to this part of the distribution are presumably nearing the end of their main-sequence lifetime and hence are the appropriate reference stars for δ Eri. It appears that Li dilution occurs as predicted for δ Eri. Boesgaard and Chesley refer δ Eri to the more Li-rich F7 dwarfs, but these stars may not have completed their depletion of Li.

The onset of dilution was probed by Alschuler (1975) who obtained Li abundances for F4 to G5 giants. Scalo, Dominy, and Pumphrey (1978) have argued that Alschuler's results are consistent with their mean red-giant mass and the predicted Li dilution factors.

e) The Weak G-Band Stars

The weak G-band stars show a large overabundance of C (Hartoog, Persson, and Aaronson 1977). Since detailed analysis of two stars shows a matching N overabundance (Cottrell and Norris 1978; Sneden *et al.* 1978) and the four stars examined for ^{13}C show a ratio $^{12}\text{C}/^{13}\text{C} \sim 4$ (Sneden *et al.* 1978), the inescapable

conclusion is that the atmospheres are severely contaminated with material which has been exposed to the CN cycle. The detailed analyses show a normal O abundance and, hence, the temperature in the processing region is sufficiently low to preclude significant equilibrium CNO-cycle processing.

The presence of Li in weak G-band stars was first noted by Dean, Lee, and O'Brien (1977). Hartoog (1978) obtained Li abundances or upper limits for 10 stars. He found an abundance near the cosmic value— $\log \epsilon(\text{Li}) = 3.0$ —for two stars. In his sample, the lower limit was $\log \epsilon(\text{Li}) \lesssim 0.8$. Sneden *et al.* obtained $\log \epsilon(\text{Li}) = 0.75$ for HR 6766. One additional star—37 Com—is included in Table 1. New observations were obtained for HR 1023 and HR 6791 which confirm the Li abundances derived by Hartoog. The model atmosphere parameters in Table 1 for HR 1023 provide a solar Al abundance from the 6696 and 6699 Å Al I lines. The Li abundance is certainly nearly cosmic for this star.

A possible model for those weak G-band stars with $\log \epsilon(\text{Li}) \lesssim 1.2$ was suggested by Sneden *et al.* (1978) and Hartoog (1978) who identified meridional currents in a rapidly rotating main-sequence star as the responsible agent. Meridional currents may deplete C and enhance N over a large zone of the star (Paczynski 1973). If these currents do not penetrate the thin Li-rich outermost layer, the star as a red giant will show a normal Li abundance (i.e., the initial—possibly depleted—abundance diluted by a factor of 60) and the low C and high N abundance of the weak G-band stars. Of course, the proposed failure of the currents to penetrate the surface also implies that the abundances of C, N, and O in the atmosphere of the rapidly rotating main-sequence star will not be perturbed. Additional theoretical work on meridional mixing is needed to investigate the possibility of excluding the mixing currents from the Li-rich surface zones. Alternatively, meridional mixing as a red giant (Sweigart and Mengel 1979) could produce a weak G-band star with a low Li abundance.

Hartoog's discovery of a nearly cosmic abundance of Li in two stars and our confirmation for HR 1023 are not consistent with the simple picture of meridional mixing. [The assumption is made that these Li-rich weak G-band stars will show a very low $^{12}\text{C}/^{13}\text{C}$ ratio (=4) as found in other weak G-band stars and are, therefore, the consequence of severe CN processing. The published $^{12}\text{C}/^{13}\text{C}$ ratio measurements refer to the less Li-rich stars.] The Li-rich stars require either a high initial abundance [$\log \epsilon(\text{Li}) \sim 5.0$] or Li to be produced internally or externally. External production via spallation reactions would not require a large fraction of the stellar luminosity (Canal, Isern, and Sanahuja 1978). However, the spallation reactions cannot produce the observed CNO abundances and the $^{12}\text{C}/^{13}\text{C}$ ratio.

Li production is possible through the chain $^3\text{He}(\alpha, \gamma)^7\text{Be}(e^-, \nu)^7\text{Li}$. Li production in weak G-band stars was suggested by Dean, Lee, and O'Brien (1977). Calculations (Sackman, Smith, and Despain 1974; Scalo, Despain, and Ulrich 1975) suggest that there

is a range of conditions (for example, see Fig. 5 of Scalo, Despain, and Ulrich) which result in a stellar surface rich in Li and the products of CN processing. However, the calculations show that the surface Li abundance is sensitive to the mixing time scales. Li abundances larger than the cosmic value can be produced; the maximum Li abundance is set by the ^3He content. Then, the fact that the maximum Li abundance for these stars is close to the cosmic value is given no significance in this interpretation.

The proposal by Sweigart and Mengel (1979) that meridional circulation in a red giant is responsible for the stars showing low $^{12}\text{C}/^{13}\text{C}$ ratios including the weak G-band stars faces a stiff test with the Li abundance estimates. Dilution of Li occurs largely before the meridional circulation becomes effective. In order for their model to explain the weak G-band stars, it must be capable of producing Li.

The meridional currents must extend down to at least the carbon shell. Nuclear lifetimes have been estimated for the middle of the carbon shell of their $1.4 M_{\odot}$ model. Reaction rates were taken from Fowler, Caughlan, and Zimmerman (1975). The ^3He lifetime is $\tau \sim 6 \times 10^4$ yr at the temperature and density of the carbon shell. The duration of the meridional mixing phase is about 54×10^6 yr. The currents require about 1×10^6 yr to move material from the carbon shell to the base of the convective envelope. Then, the material will be circulated about 20 times through the C shell. Clearly, the ^3He content of the envelope will be converted to ^7Be . However, the lifetime of the ^7Be is very short; $\tau \sim 9$ yr for $^7\text{Be}(p, \gamma)^8\text{B}$ and ~ 30 yr for $^7\text{Be}(e^-, \nu)^7\text{Li}$ assuming that the Be ions are fully ionized. The ^7Li lifetime is much less than 1 yr. With a circulation velocity $V_{\text{EV}} = 2.4 \times 10^{-3}$ cm s $^{-1}$ in the carbon shell, the ^7Be and ^7Li are destroyed near the production site and ^7Li is not carried to the surface.

The much higher velocities associated with convective motions appear to be essential if ^7Li is to be produced. Sweigart and Mengel argue that meridional circulation in a red giant is responsible for the weak G-band stars. The high Li abundances seen in these stars indicate that their explanation is incomplete. It remains to be shown how the necessary conditions for mixing and processing are attained in the post-main-sequence evolution of these relatively low-mass and low-luminosity stars.

V. CONCLUDING REMARKS

Thanks to the existence of several destruction, dilution, and production mechanisms affecting the surface Li abundance of a red giant, a detailed nucleosynthetic accounting for this light element is not yet possible. This study has provided several new results.

The first result is that the more massive stars ($m \gtrsim 1.2 M_{\odot}$) can evolve as predicted by standard sequences of stellar models, i.e., [$\log \epsilon(\text{Li}) = 1.2$ to -0.5] and the $^{12}\text{C}/^{13}\text{C}$ (~ 25) ratio match the model predictions (see Fig. 9). This implies that the average mass-loss rate is low prior to the red-giant phase and

that the depth of the Li-rich skin around the main-sequence star is predicted correctly. Mass loss may be the origin of the lower Li abundances seen in some supergiants.

With the notable exception of the weak G-band stars, the low $^{12}\text{C}/^{13}\text{C}$ ratio giants show a lower Li abundance than the great majority of the normal $^{12}\text{C}/^{13}\text{C}$ giants. This result serves to exclude spallation reactions as the mechanism responsible for the high ^{13}C content. On the assumption that the Li depletion on the main sequence is a single-valued function of the stellar mass, the Li- $^{12}\text{C}/^{13}\text{C}$ correlation suggests a mass limit $m < 1.3 M_{\odot}$ for the low $^{12}\text{C}/^{13}\text{C}$ ratio stars. Addition of CN-cycle processed material would explain the low Li abundance seen in these ^{13}C rich stars. The mass limit is consistent with the hypothesis that mixing is induced by either a strong He core flash or meridional mixing in a red giant with a rapidly rotating core.

In the weak G-band stars, the Li abundance ranges up to about the cosmic value. Li production appears to be necessary. Meridional circulation is unlikely to be able to explain these stars because the circulation velocities are too small. It would be of great interest to obtain abundances for other critically important elements (e.g., Be, ^{17}O , and ^{18}O) in order to define the production phase and to search for correlations between Li, ^{12}C , ^{13}C , ^{14}N , and other key isotopes.

One event in the evolution of low-mass stars may possibly explain both the normal and the weak G-band stars with low $^{12}\text{C}/^{13}\text{C}$ ratios. Two alternative scenarios may be suggested. First, CN-processed material is continuously added to the surface during the event; the Li abundance initially decreases and only increases after the surface has reached the $^{12}\text{C}/^{13}\text{C} \sim 4$ condition. The keys to this scenario are the time scale for exposure of the material to high temperatures (the ^7Be and ^7Li are easily destroyed) and the duration of the event. In the second scenario, different stars are subject to events of differing severity. In some stars, the conditions attained lead to Li destruction and a low $^{12}\text{C}/^{13}\text{C}$ giant results. In

the progenitors of the weak G-band stars, the conditions must differ so that C is depleted and Li is produced. The He core flash in low-mass stars is a potential example of this type of event. The strength of the flash and hence the degree of possible mixing is mass dependent. Unfortunately it is currently uncertain whether the He core flash leads to mixing.

Additional observations of Li will surely be required before the history of red giants is unraveled. Li abundances for a larger and carefully selected sample of G and K giants and subgiants should provide answers to certain key questions; e.g., Are giants with a normal $^{12}\text{C}/^{13}\text{C}$ ratio and a low Li abundance rare as suggested by Figure 9? If none are found, the present conclusion will be confirmed: stars with $m \lesssim 1 M_{\odot}$ evolve to become red giants with a low $^{12}\text{C}/^{13}\text{C}$ ratio. A large sample will also reveal whether stars exist with a Li abundance and a $^{12}\text{C}/^{13}\text{C}$ ratio between those displayed by the weak G-band stars and the majority of the G and K giants.

The Li and $^{12}\text{C}/^{13}\text{C}$ comparison should be extended to cover M giants and supergiants. The blending of TiO lines are important in these stars, but spectrum synthesis techniques allow these blends to be taken into account. Finally, application of the new digital detectors to a reinvestigation of the Li abundance in main-sequence stars should not be overlooked. Some of the observational questions will be answered in later papers in this series.

Our interest in lithium in giants was kindled by Professor G. Wallerstein's suggestion that Li could serve to test the spallation hypothesis for low $^{12}\text{C}/^{13}\text{C}$ giants. We thank him for this suggestion. We wish to thank Dr. J. Scalo for helpful discussions and a thorough review of a draft of the paper, Dr. G. Smith for a list of Ca g -values, Dr. J. Tomkin for his enthusiastic support, and Dr. R. E. Luck for advice on spectrum synthesis techniques. Our research has been supported in part by the National Science Foundation (grants AST 75-21803 and 77-23213) and the Robert A. Welch Foundation of Houston, Texas.

REFERENCES

- Alschuler, W. R. 1975, *Ap. J.*, **195**, 649.
 Audouze, J. 1970, *Astr. Ap.*, **8**, 436.
 Auman, J., and Woodrow, J. E. J. 1975, *Ap. J.*, **197**, 163.
 Bell, R. A., Eriksson, K., Gustafsson, B., and Nordlund, A. 1976, *Astr. Ap. Supp.*, **23**, 37.
 Bodenheimer, P. 1965, *Ap. J.*, **142**, 451.
 Boesgaard, A. M. 1970, *Ap. Letters*, **5**, 145.
 ———. 1971, *Ap. J.*, **167**, 511.
 ———. 1976a, *Pub. A.S.P.*, **88**, 353.
 ———. 1976b, *Ap. J.*, **210**, 466.
 Boesgaard, A. M., and Chesley, S. E. 1976, *Ap. J.*, **210**, 475.
 Boesgaard, A. M., Heacox, W. D., and Conti, P. S. 1977, *Ap. J.*, **214**, 124.
 Bonsack, W. K. 1959, *Ap. J.*, **130**, 843.
 Branch, D. 1979, *M.N.R.A.S.*, **187**, 9P.
 Cameron, A. G. W. 1955, *Ap. J.*, **121**, 144.
 Cameron, A. G. W., and Fowler, W. A. 1971, *Ap. J.*, **164**, 111.
 Canal, R., Isern, J., and Sanahuja, B. 1978, *Ap. J.*, **220**, 606.
 Cottrell, P. L., and Norris, J. 1978, *Ap. J.*, **221**, 893.
 Dean, G. A., Lee, P., and O'Brien, A. 1977, *Pub. A.S.P.*, **89**, 222.
 Dearborn, D. S. P., Tinsley, B. M., and Schramm, D. N. 1978, *Ap. J.*, **223**, 557.
 Fowler, W. A., Caughlan, G. R., and Zimmerman, B. A. 1975, *Ann. Rev. Astr. Ap.*, **13**, 69.
 Gornik, W., Kaiser, D., Lange, W., Luther, J., Meier, K., Radloff, H.-H., and Schulz, H.-H. 1973, *Phys. Letters*, **45A**, 219.
 Gustafsson, B., Kjaergaard, P., and Andersen, S. 1974, *Astr. Ap.*, **34**, 99.
 Hansen, L., and Kjaergaard, P. 1971, *Astr. Ap.*, **15**, 123.
 Hartoog, M. A. 1978, *Pub. A.S.P.*, **90**, 167.
 Hartoog, M. R., Persson, S. E., and Aaronson, M. 1977, *Pub. A.S.P.*, **89**, 660.
 Herbig, G. H. 1965, *Ap. J.*, **141**, 588.
 Herbig, G. H., and Wolff, R. J. 1966, *Ann. d'Ap.*, **29**, 593.
 Iben, I. 1964, *Ap. J.*, **140**, 1631.
 ———. 1965, *Ap. J.*, **142**, 1447.
 ———. 1966, *Ap. J.*, **143**, 483.
 ———. 1967a, *Ap. J.*, **147**, 624.
 ———. 1967b, *Ap. J.*, **147**, 650.
 Kurucz, R. L., and Peytremann, E. 1975, *Smithsonian Ap. Obs., Spec. Rept.* No. 362.

- Lambert, D. L. 1976, *Mém. Soc. Roy. Sci. Liège*, 6^e sér., **9**, 405.
- Lambert, D. L., and Luck, R. E. 1978, *M.N.R.A.S.*, **183**, 79.
- Lambert, D. L., and Ries, L. M. 1977, *Ap. J.*, **217**, 508.
- Luck, R. E. 1977, *Ap. J.*, **218**, 752.
- . 1978, *Ap. J.*, **219**, 148.
- Miller, G. E., and Scalo, J. M. 1979, *Ap. J. Suppl.*, **41**, 513.
- Paczynski, B. 1973, *Acta Astr.*, **23**, 191.
- Ramsey, L. W. 1977, *Ap. J.*, **215**, 827.
- Reeves, H. 1974, *Ann. Rev. Astr. Ap.*, **12**, 437.
- Sackmann, I. J., Smith, R. L., and Despain, K. H. 1974, *Ap. J.*, **187**, 555.
- Scalo, J., Despain, K., and Ulrich, R. 1975, *Ap. J.*, **196**, 805.
- Scalo, J. M., Dominy, J. F., and Pumphrey, W. A. 1978, *Ap. J.*, **221**, 616.
- Scalo, J. M., and Miller, G. E. 1978, *Ap. J.*, **225**, 523.
- Schatzman, E. 1977, *Astr. Ap.*, **56**, 211.
- Smith, G. 1978, private communication.
- Smith, G., and O'Neill, J. 1975, *Astr. Ap.*, **38**, 1.
- Snedden, C., Lambert, D. L., Tomkin, J., and Peterson, R. 1978, *Ap. J.*, **222**, 585.
- Sweigart, A. V., and Mengel, J. G. 1979, *Ap. J.*, **229**, 624.
- Tomkin, J., Luck, R. E., and Lambert, D. L. 1976, *Ap. J.*, **210**, 694.
- van den Heuvel, E. P. J. 1975, *Ap. J. (Letters)*, **196**, L121.
- Vauclair, S., Vauclair, G., Schatzman, E., and Michaud, G. 1978, *Ap. J.*, **223**, 567.
- Vogt, S. S., Tull, R. G., and Kelton, P. K. 1978, *Appl. Optics*, **17**, 574.
- Wallerstein, G. 1966, *Ap. J.*, **143**, 823.
- . 1975, private communication.
- Wallerstein, G., and Conti, P. S. 1969, *Ann. Rev. Astr. Ap.*, **7**, 69.
- Weymann, R., and Sears, R. L. 1965, *Ap. J.*, **142**, 174.
- Williams, P. M. 1971, *M.N.R.A.S.*, **153**, 171.
- . 1972a, *M.N.R.A.S.*, **155**, 17P.
- . 1972b, *M.N.R.A.S.*, **158**, 361.
- Zappala, R. R. 1972, *Ap. J.*, **172**, 57.

JAMES F. DOMINY and DAVID L. LAMBERT: Department of Astronomy, University of Texas, Austin, TX 78712

SVEIN SIVERTSEN: Institute for Mathematical & Physical Sciences, University of Tromsø, P.O. Box 953, N-9001 Tromsø, Norway